

# Effect of cations on the hydrated proton

Niklas Ottosson<sup>†,\*</sup>, Johannes Hunger<sup>‡</sup>, Huib. J. Bakker<sup>†,\*</sup>

<sup>†</sup>FOM Institute AMOLF, Science Park 104, 1098 XG Amsterdam, The Netherlands

<sup>‡</sup>Molecular Spectroscopy Department, Max Planck Institute for Polymer Research, Ackermannweg 10, 55128 Mainz, Germany

**ABSTRACT:** We report on a strong non-additive effect of protons and other cations on the structural dynamics of liquid water, which is revealed using dielectric relaxation spectroscopy in the frequency range of 1-50 GHz. For pure acid solutions, protons are known to have a strong structuring effect on water, leading to a pronounced decrease of the dielectric response. We observe that this structuring is reduced when protons are co-solvated with salts. This reduction is exclusively observed for combinations of protons with other ions; for all studied solutions of co-solvated salts the effect on the structural dynamics of water is observed to be purely additive, even up to high concentrations. We derive an empirical model that quantitatively describes the non-additive effect of co-solvated protons and cations. We argue that the effect can be explained from the special character of the proton in water and that Coulomb fields exerted by other cations, in particular doubly charged cations like  $\text{Mg}^{2+}_{\text{aq}}$  and  $\text{Ca}^{2+}_{\text{aq}}$ , induce a localization of the  $\text{H}^+_{\text{aq}}$  hydration structures.

The hydrated excess proton behaves radically different from other ions in water. It can go in and out of existence via water's autolysis reaction,  $\text{H}_2\text{O}_{\text{aq}} \rightleftharpoons \text{H}^+_{\text{aq}} + \text{OH}^-_{\text{aq}}$ , and its structural and dynamic properties are intimately linked with the topology of the hydrogen (H) bonding network of the water solvent.<sup>1</sup> While the transport of ordinary hydrated ions proceeds via diffusion of the ion's full mass, the Grotthuss transport mechanism of the proton, on the other hand, requires relatively small nuclear rearrangements to move the protonic charge over large distances.<sup>2,3</sup> This is possible due to efficient electron-transfer reactions between the protonic hydration structure and its first solvation shell, thereby enabling a near barrier-free interconversion between the limiting Eigen ( $\text{H}_9\text{O}_4^+$ )<sub>aq</sub> and Zundel ( $\text{H}_5\text{O}_2^+$ )<sub>aq</sub> complexes.<sup>4,5</sup>

In many aqueous systems, e.g. intracellular water and proton exchange membranes, aqueous proton transfer takes place in the presence of other ionic co-solutes at high concentrations. From structure-determining experiments, such as X-ray and neutron diffraction,<sup>6</sup> extended X-ray absorption fine-structure (EXAFS) and large-angle X-ray scattering (LAXS)<sup>7</sup> it is known that the radial distributions of hydrated ions, especially those of higher valency, show substantial spatial structure extending well beyond the first solvation shell. This makes the H-bond topology of the electrolyte solution different from that of pure water. Furthermore, NMR,<sup>8</sup> dielectric relaxation,<sup>9,10,11</sup> ultrafast mid-infrared pump-probe studies<sup>12,13</sup> and MD simulations<sup>14</sup> have shown that the dynamics of water

molecules hydrating ionic species can be severely slowed down. Since the structural diffusion of the proton is dependent on both the water structure and its reorientation dynamics, it is expected that the conduction mechanism and mobility of the proton will be affected by other ionic co-solutes.

In this work we investigate how the hydration and transport mechanism of the proton are affected by the co-solvation of salts composed of mono-atomic ions using dielectric spectroscopy in the GHz frequency range. This technique is a powerful tool in studying the reorientation dynamics of liquids of small polar molecules.<sup>15,16</sup> Through measurements of the complex permittivity,  $\hat{\epsilon}(\nu) = \epsilon'(\nu) - i\epsilon''(\nu)$ , reflecting the sample's macroscopic polarization as a function of the field frequency,  $\nu$ , information about the reorientation dynamics of the permanent electric dipoles of water molecules can be extracted. The pronounced dispersion in  $\hat{\epsilon}(\nu)$  of water in this frequency range is well described by a Debye relaxation model, with a Debye relaxation time  $\tau_D$  of  $\sim 8.7$  ps.<sup>17</sup>

Complex permittivity spectra in the range of 1-50 GHz were measured at  $22 \pm 0.5$  °C using a phase-sensitive vector network analyzer (VNA, Rhode-Schwartz model ZVA67) together with a home-built reflectometric cell for liquid samples. The setup and approach has been described elsewhere<sup>18,19</sup> and additional experimental details are given in the SI.

We study ternary aqueous salt solutions with  $\text{Cl}^-$  as the common anion. In a first set of experiments, all solutions were prepared such that the cation/proton ratio was varied while keeping the  $\text{Cl}^-$  concentration constant at 1 mol/L. Figure 1 shows the measured frequency dependent complex permittivity (circles) of these mixtures. The main panels zoom in on the dominant water Debye relaxation mode, while the insets show overview spectra ranging from 1-50 GHz (note that the conductivity contributions have been removed for visual clarity. The corresponding raw data and their decomposition into relaxation and conductivity contributions are given in the SI). In panel a) we show data for ternary mixtures of water,  $\text{MgCl}_2$ , and HCl, ranging from 0.5 mol/L  $\text{MgCl}_2$  to 1 mol/L HCl, over intermediate mixtures. We fitted the permittivity spectra of all investigated electrolytes with a single Cole-Cole relaxation mode<sup>16</sup> and a conductivity term (see SI for details), i.e. to the following expression:

$$\hat{\epsilon}(\nu) = \frac{S}{1 + (i2\pi\nu\tau)^{1-\alpha}} + \epsilon_\infty - \frac{i\sigma}{2\pi\nu\epsilon_0} \quad (1)$$

where  $S = \epsilon_S - \epsilon_\infty$  is the dielectric strength in which  $\epsilon_S$  and  $\epsilon_\infty$  gives the static dielectric constant and the limiting permittivity at high frequencies, respectively. Furthermore the

$\alpha$ -parameter describes the spectral broadening (in the limit  $\alpha=0$  a Cole-Cole relaxation mode becomes a Debye mode),  $\sigma$  is the solution conductivity and  $\epsilon_0$  is the permittivity of free space. The lines in Fig.1 show the results of least-square fits. The obtained relaxation times are slightly lower (1-2%) than for bulk water, as is commonly observed for aqueous inorganic electrolytes.<sup>9,20</sup> An interesting observation is that the amplitude of the dielectric response shows a clear nonlinear dependence on the composition for the  $H^+/Mg^{2+}$  mixtures. This nonlinearity is not observed for the  $Cs^+/Mg^{2+}$  mixtures.

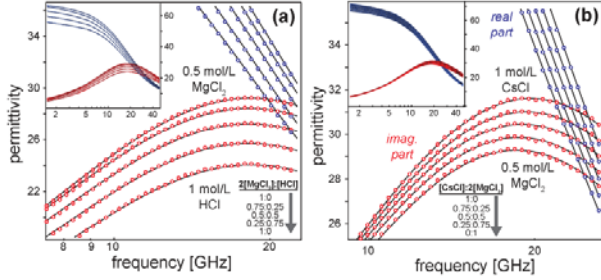


**Figure 1)** Complex permittivity spectra of a) aqueous mixtures of  $HCl/MgCl_2$  and b) mixtures of  $CsCl/MgCl_2$  at a constant  $Cl^-$  concentration of 1 mol/L. Solid lines are fits to Eq. 1.

As commonly observed for electrolytes, all dielectric strengths  $S$  here measured are smaller than that of pure water; this effect is commonly referred to as depolarization.<sup>10</sup> Since dilution of the water solvent by ions is a trivial (and small) contribution we correct for this by defining the depolarization as  $\Delta S = S_n - S$ . Here  $S_n$  is the water density corrected dielectric response that would nominally be expected if the reorientational freedom of the water molecules in the solution was the same as that of pure water.<sup>21</sup>

The fact that the depolarization effect is considerable for electrolytes arises from two different effects. One of these is kinetic depolarization, originating from the coupling of the ion translation in the external electric field to the rotational motion of the solvent.<sup>10</sup> The resulting rotational polarization current is opposite to the current resulting from the rotational motion of the solvent itself.<sup>22,23</sup> The remaining part of the depolarization can be assigned to irrotational binding of the water dipoles by the ionic solutes.<sup>24</sup>

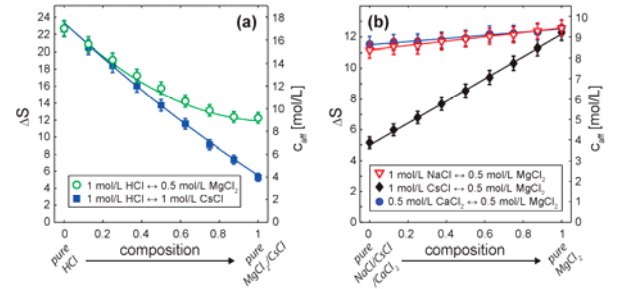
The depolarization can be related to an 'affected' water concentration,  $c_{aff}$ , as the difference between the actual water concentration in the sample,  $c$ , and the concentration of 'detected' water molecules,  $c_{det}$ , i.e. which gives rise to dielectric relaxation.  $c_{aff}$  can be seen as a subset of molecules whose rotation is strongly hindered upon the dissolution of the ionic solutes, as found in several studies.<sup>25,26</sup> Using the Cavell equation<sup>29</sup> we can determine  $c_{det}$  from the measured dielectric strength  $S$  and thus obtain  $c_{aff}$  via the following expression

$$c_{aff} = c - c_{det} = c - S \times \frac{2\epsilon_S + 1}{\epsilon_S} \times \frac{k_B T \epsilon_0}{N_A g \mu^2} \approx \frac{c_0}{S_0} \times \Delta S \quad (2)$$

where  $k_B$  is Boltzmann's constant,  $T$  is the solution temperature,  $N_A$  is Avogadro's number,  $\mu$  is the water molecule dipole moment and  $g$  is the Kirkwood correlation factor. The approximation made in Eq. 2 (where  $S_0 \approx 73.5$  and  $c_0 \approx 55.4$  mol/L are the dielectric strengths and  $H_2O$  concentrations of the pure water solvent) is justified for aqueous solutions since the local field correction factor  $(2\epsilon_S + 1)/\epsilon_S$  is nearly

constantly equal to 2 for these strong dielectrics. Furthermore, we assume that the effective dipole moment  $\mu_{eff} = \sqrt{g}\mu$  of water molecules contributing to the dielectric response is the same as that of pure water, which has been shown to be a valid assumption for aqueous electrolytes at ambient conditions.<sup>11,27,28</sup> Due to the direct proportionality of  $\Delta S$  to  $c_{aff}$ , as given by Eq. 2, we will present the data throughout the remainder of this paper using two different axes, one pertaining to each of the two quantities.

Figure 2 shows measured  $\Delta S$  values (left-hand vertical axis) together with derived  $c_{aff}$  values (right-hand vertical axis) for various mixed electrolytes at constant 1 mol/L  $Cl^-$  concentration. Panel a) displays data for two acid-salt mixtures,  $HCl/CsCl$  (solid blue squares) and  $HCl/MgCl_2$  (open green circles). Remarkably, there is a notable non-linearity in the depolarization across the composition range for the  $HCl/MgCl_2$  mixtures. While the initial decrease of  $\Delta S$  upon replacing protons with (half the amount of)  $Mg^{2+}$  is large, the decrement per  $Mg^{2+}$  is gradually becoming smaller as the mixture composition approaches pure  $MgCl_2$  (note that this is also directly visible from the non-linear decrement in  $\epsilon''(v)$  in the raw data of Fig. 1a). A non-linearity is also discernible in the data of the  $HCl/CsCl$  mixtures, although much less pronounced in comparison to the  $HCl/MgCl_2$  data.



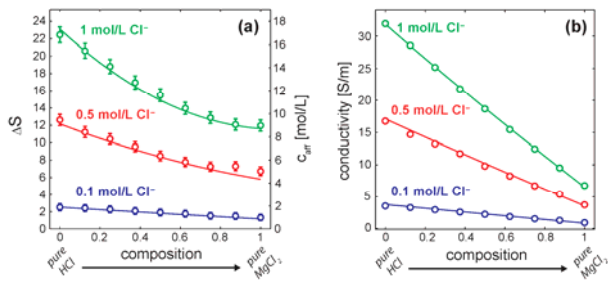
**Figure 2)** Depolarization  $\Delta S$  (left-hand vertical axis) and concentration  $c_{aff}$  of water molecules missing from the dielectric response (right-hand vertical axis) for various mixed a) salt-acid and b) salt-salt electrolytes. For all solutions the  $Cl^-$  concentration is constant at 1 mol/L. Solid lines are least square fits to the models discussed in the main text.

Figure 2b) shows data for mixtures of  $NaCl/MgCl_2$  (open red triangles),  $CsCl/MgCl_2$  (solid black diamonds), and  $CaCl_2/MgCl_2$  (solid blue circles), all at 1 mol/L  $Cl^-$  concentration. In sharp contrast to the acid/salt mixture data in panel a), the depolarization for the  $CsCl/MgCl_2$ ,  $NaCl/MgCl_2$  and  $CaCl_2/MgCl_2$  mixtures interpolate linearly between the limiting cases of pure aqueous 1 mol/L  $CsCl$ , 1 mol/L  $NaCl$ , 0.5 mol/L  $CaCl_2$  and 0.5 mol/L  $MgCl_2$ , i.e. a global model of the form  $\Delta S = A[XCl_n] + B[MgCl_2]$ , excellently describes the data ( $X = Na, Cs$  or  $Ca$ ), as seen from the solid lines given together with the data in the figure. Hence, for salt-salt mixtures, the effect on the water dynamics appears to be perfectly additive.

The depolarization values of the acid-salt mixtures are consistently lower than expected from assuming additive hydration dynamics of the proton and salt cation. The fact that  $\Delta S$  deviates maximally from the linear expectation when the composition parameter is close to 0.5, i.e. when both species are present at high concentrations, suggests the existence of a cooperative effect of the proton and the co-solvated salt cation on the dynamics of water.

We have performed further experiments for two other  $\text{MgCl}_2/\text{HCl}$  mixture series at various total  $\text{Cl}^-$  concentrations (but keeping it constant within each series). The circles in Fig. 3a) shows depolarizations of solutions at 0.1 mol/L (blue), 0.5 mol/L (red), and 1 mol/L  $\text{Cl}^-$  concentration (green). Interestingly, the non-linear behavior shows a marked concentration dependence: At 0.1 mol/L  $\text{Cl}^-$  concentration  $\Delta S$  is linearly interpolating between the limiting pure acid and pure salt cases, while deviations from this ideal behavior become pronounced upon going to 0.5 and 1 mol/L.

Within the Hubbard-Onsager model the magnitude of the kinetic depolarization effect is proportional to the electrolyte conductivity.<sup>22,23</sup> Thus, it is of interest to establish whether the observed non-linearity in the depolarization is associated with a corresponding non-linearity in the electrolyte conductivities. As can be seen in Fig. 3b) this is not the case, and the effects of protons and ions on the conductivity of the mixtures are close to additive. The conductivities of all the solutions plotted in Fig. 3 can be fitted quite well to a simple Kohlrausch's law<sup>31,32</sup> given by the solid lines (see SI for details). We also note that the conductivity values for aqueous  $\text{MgCl}_2$  and  $\text{HCl}$  electrolytes are in good agreement with previous literature values.<sup>33,34</sup> Interestingly, this is in agreement with the MD simulation study of Xu *et al.*<sup>35</sup> who found that the conductivity contribution of  $\text{HCl}$  and added salt ions are close to additive.



**Figure 3)** Panel a) shows experimental values (open circles) and global fits to Eq. 3 (solid lines) of  $\Delta S$  and  $c_{\text{eff}}$  for mixed  $\text{HCl}/\text{MgCl}_2$  electrolytes while panel b) shows the conductivity of the same solutions (fitting procedure described in SI).

The presence of a cooperative effect upon co-solvation of the proton and salt cations implies a reduction of the increments  $\partial\Delta S/\partial[\text{HCl}]$  upon adding a salt  $\text{XCl}_n$  to a pure  $\text{HCl}$  solution. We have performed additional experiments on solutions with and without a fixed concentration of 0.25 mol/L  $\text{MgCl}_2$  (or  $\text{HCl}$ ) and a variable concentration of  $\text{HCl}$  (or  $\text{MgCl}_2$ ); the data are given in Fig. 4. The blue circles in panel a) give  $\Delta S$  as function of concentration of pure  $\text{HCl}$  solutions; the data are nearly linear with a weak tendency to level off at higher concentrations – something to which we will return shortly. If the hydration dynamics of  $\text{HCl}$  and  $\text{MgCl}_2$  would be additive, one would expect the presence of 0.25 mol/L  $\text{MgCl}_2$  to merely positively offset the curve, as illustrated by the dashed blue line. However, the experimental data (red circles) look strikingly different: The slope  $\partial\Delta S/\partial[\text{HCl}]$  is much smaller than what would be expected if the effects of  $\text{Mg}^{2+}$  and  $\text{H}^+$  on the water mobility were additive. This provides further evidence that the effect of  $\text{Mg}^{2+}$  and  $\text{H}^+$  on the orientational mobility of water upon co-solvation is suppressed compared to the effect of the respective ions in pure (binary) systems.

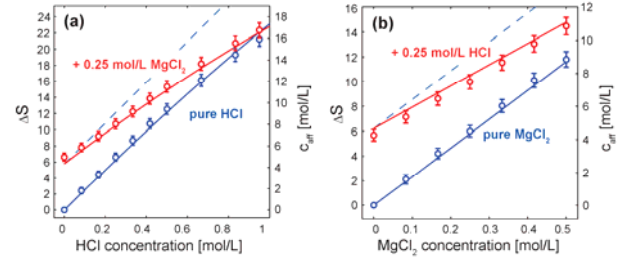


**Figure 4)** Panel a) shows  $\Delta S$  and  $c_{\text{eff}}$  for pure  $\text{HCl}$  solutions (blue circles) and for solutions in which a fixed concentration of 0.25 mol/L  $\text{MgCl}_2$  was added (red circles). Panel b) shows data for the reversed situation, i.e.  $\text{MgCl}_2$  solutions (blue circles) and those to which 0.25 mol/L  $\text{HCl}$  was added (red circles). The dashed blue lines show the prediction from an additive model. The solid lines are the result of a global fit to Eq. 3.

Notably, the cooperative effect does not seem to be directly related to the nature of the anion as experiments for  $\text{HClO}_4/\text{Mg}(\text{ClO}_4)_2$  mixtures give nearly identical results as for the chloride containing electrolytes (see SI). Thus, having established that the non-additivity of the depolarization is primarily dependent on the concentrations of the salt cation  $\text{X}^{n+}$  and proton, we have found the depolarization of mixed acid-salt solutions to be well described by the expression:

$$\Delta S = A[\text{X}^{n+}] + B[\text{H}^+] - C[\text{X}^{n+}][\text{H}^+] - D[\text{H}^+]^2$$

This equation yields good fits to all data over a large range of concentrations and composition ratios. Within the framework of Eq. 2, A and B can be interpreted as the individual effects the cations and protons have on reducing the rotational mobility of water molecules while C gives the strength the cooperative interaction of protons and cations on the water response. The (small) D-term term similarly accounts for negative deviations at high proton concentrations. The solid lines shown in Figs. 3 and 4 are the result of a global fit to the data in all panels, with fit parameters  $A = 25$ ,  $B = 23$ ,  $C = 24$  L/mol and  $D = 3$  L/mol. We find a similar deviation from additivity for mixtures of  $\text{CaCl}_2/\text{HCl}$  as for mixtures of  $\text{MgCl}_2/\text{HCl}$  (see SI), while it is much less pronounced for salts of monovalent cations; a fit to Eq. 3 for  $\text{CsCl}/\text{HCl}$  mixtures gives  $B = 5$  and much weaker non-linear term,  $C = 4$  L/mol, notably of similar magnitude as  $D = 3$  L/mol (see SI). This observation leads us to conclude that the charge of the cation co-solvated with  $\text{H}^+_{\text{aq}}$  is the most important factor in decreasing the depolarization effect of  $\text{H}^+_{\text{aq}}$ .

In identifying the origin of the observed non-additive effect of co-solvated proton and cations on the dielectric response of water, it should be noted that the molar dielectric decrement,  $\partial\Delta S/\partial[\text{H}^+]$ , associated with the proton in binary solutions is exceptionally large ( $\sim 23$ - $24$  mol<sup>-1</sup>) and corresponds to 18-19 affected water molecules per  $\text{H}^+$ . Using the model of Hubbard and Onsager,<sup>22,23</sup> the majority of the effect ( $\sim 15$  water molecules) has been thought to originate from kinetic depolarization,<sup>30</sup> arising due to the exceptionally large mobility of the proton. However, the sub-division into static and dynamic effects is less clear for the proton than for other ions as the limiting hydration structures are very short-lived and continuously undergoes ultrafast structural reorganization on sub-ps timescales. The dynamic hydration shell of the

proton is furthermore unusually extended, encompassing as much as three hydration layers, in which a significant amount of water molecules align their dipole moments in anti-parallel configurations.<sup>36</sup> The depolarization of the water response due to protons may thus largely find its origin in the stiffening of the hydrogen bonds in the (transient) hydration structures and the local reduction of the Kirkwood dipole correlation factor  $g$  due to the different arrangement of the water molecules compared to bulk liquid water, for which  $g$  is as large as  $\sim 2.7$ .<sup>17</sup>

The presence of highly charged cations will tend to reduce the delocalization of the proton charge as a result of Coulomb repulsion, thereby weakening several of the originally strong hydrogen bonds within the proton hydration structure. As a result, the co-solvated cations will induce a mobilization of the water molecules and thereby increase the overall dielectric response, i.e. reduce  $\Delta S$ . The reduction of the spatial extent of the proton hydration structure also reduce the volume over which the Kirkwood dipole correlation factor is decreased in comparison to bulk water, thus further enhancing the polarization response, i.e. decreasing  $\Delta S$ . The spatial extent of the proton hydration structure can also be reduced upon the formation of special proton-proton ion pairs as found in MD simulations of moderately concentrated HCl solutions,<sup>35,37</sup> and which will further decrease  $\Delta S$ .

The here observed non-additive effect of small and highly charged cations on the depolarization of water induced by protons is thus likely the result of the diffuse nature of the protonic charge. This makes hydrated protons structure and their effects on the polarization response susceptible to the Coulomb field exerted by other ions. For other cations the charge is highly localized and thus their effects are additive, as found in all experiments on salt-salt mixtures (see Fig. 2b).

We hope that the present observations will inspire future *ab initio* MD simulations that explicitly describe the structural diffusion of the hydrated proton in the presence co-solvated salts. Such simulations may provide a complete mechanistic understanding of the non-additive effect of protons and cations on the polarization response of water unraveled here.

## ASSOCIATED CONTENT

### Supporting Information

Additional experimental details and supplementary DRS and conductivity data. This material is available free of charge via the Internet at <http://pubs.acs.org>.

## AUTHOR INFORMATION

### Corresponding Authors

\*n.ottosson@amolf.nl and h.bakker@amolf.nl

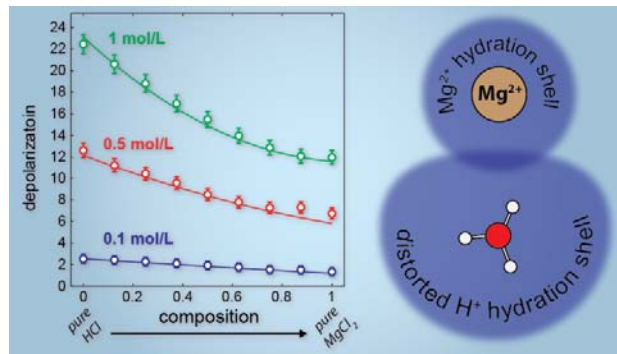
## ACKNOWLEDGMENT

This work is part of the research program of the Stichting voor Fundamenteel Onderzoek der Materie (FOM) which is financially supported by the Nederlandse organisatie voor Wetenschappelijk Onderzoek (NWO). The authors thanks H. Schoenmaker and H. J. Boluijt for technical support. N.O. gratefully acknowledges the European Commission (FP7) for funding through the award of a Marie Curie fellowship.

## REFERENCES

- (1) Marx, D. *ChemPhysChem*, 2006, 7, 1848-1870.
- (2) Agmon, N. *Chem. Phys. Lett.*, 1995, 244, 456-462.
- (3) Cukierman, S. *Et Biochimica et Biophysica Acta (BBA) - Bioenergetics*, 2006, 1757, 876-885.
- (4) Marx, D.; Tuckerman, M.E.; Hutter, J.; Parrinello, M. *Nature*, 1999, 397, 601-604.
- (5) Schmitt, U.W.; Voth, G.A. *J. Chem. Phys.*, 1999, 111, 9361-9381.
- (6) Bowron, D.T.; Beret, E.C.; Martin-Zamora, E.; Soper, A.K.; Sánchez Marcos, E. *J. Am. Chem. Soc.*, 2012, 134, 962-967.
- (7) Jalilehvand, F.; Spångberg D.; Lindqvist-Reis, P.; Hermansson, K.; Persson, I.; Sandström, M. *J. Am. Chem. Soc.*, 2001, 123, 431-441.
- (8) Endom, L.; Hertz, H.G.; Thul, B.; Zeidler, M.D. *Ber. Buns. Gesell.*, 1967, 71, 1008-1031.
- (9) Haggis, G.H.; Hasted, J.B.; Buchanan, T.J. *J. Chem. Phys.*, 1952, 20, 1452.
- (10) Kaatzte, U. *Z. Phys. Chem.*, 1983, 135, 51-75.
- (11) Buchner, R.; Hefter, *Phys.Chem.Chem.Phys.*, 2009, 11, 8984-8999.
- (12) Kropman, M.F.; Bakker, H.J. *Science*, 2001, 291, 2118-2120.
- (13) Tielrooij, K. J.; Garcia-Araez, N.; Bonn, M.; Bakker, H.J. *Science*, 2010, 328, 1006-1009.
- (14) Laage, D.; Stirnemann, G.; Sterpone, F.; Rey, R.; Hynes, J. T. *Ann. Rev. Phys. Chem.*, 2011, 62, 395-416.
- (15) Böttcher, C. J. F.; Bordewijk, P. *Theory of Electric Polarization Vol. 1 & 2*, Elsevier Scientific Pub. Co., Amsterdam and New York (1978)
- (16) Kremer, F.; Schönhals, A. *Broadband Dielectric Spectroscopy*, Springer Verlag, Berlin (2002)
- (17) Buchner, R.; Barthel, J.; Stauber, J. *Chem. Phys. Lett.* 1999, 306, 57-63.
- (18) Blackham, D.V.; Pollard, R.D. *IEEE Trans. Instrum. Meas.*, 1997, 46, 1093-1099.
- (19) Ensing, W.; Hunger, J.; Ottosson, N.; Bakker, H.J. *J. Phys. Chem. C*, 2013, 117, 12930-12935.
- (20) Wachter, W.; Kunz, W.; Buchner, R.; Hefter, G. J. *Phys. Chem. A*, 2005, 109, 8675-8683.
- (21)  $S_n$  is calculated from the sample water content using the Cavell equation [E.A.S. Cavell et al. *Trans. Faraday Soc.*, 1971, 67, 2225].
- (22) Hubbard, J.; Onsager, L. *J. Chem. Phys.*, 1977, 67, 4850.
- (23) Hubbard, J.; Onsager, L.; v. Beek, W.M.; Mandel, M. *Proc. Nat. Ac. Sci.* 1977, 74, 401.
- (24) Barthel, J.; Buchner, R.; Bachhuber, K.; Hetzenauer, H.; Kleebauer, M.; Ortmaier, H. *Pure & Appl. Chem.*, 1990, 62, 2287-2296.
- (25) Verde, A.V.; Lipowsky, R. *J. Phys. Chem. B*, 2013, 117, 10556-10566.
- (26) Stirnemann, G.; Wernersson, E.; Jungwirth, P.; Laage, D. *J. Am. Chem. Soc.*, 2013, 135, 11824-11831.
- (27) Maribo-Mogensen, B.; Kontogeorgis, G.M.; Thomsen, K. *J. Phys. Chem. B*, 2013, 117, 10523-10533.
- (28) Kaatzte, U. *J. Mol. Liq.*, 2011, 162, 105-112.
- (29) Cavell, E.A.S.; Knight, P.C.; Sheikh, M.A. *Trans. Faraday Soc.*, 1971, 67, 2225.
- (30) Tielrooij, K.J.; Timmer, R.L.A.; Bakker, H.J.; Bonn, M. *Phys. Rev. Lett.*, 2009, 102, 198303.
- (31) M. Robson-Wright, *An Introduction to Aqueous Electrolyte Solutions*, Wiley (2007).
- (32) While the present concentrations are beyond the validity range of Kohlrausch's law, satisfactory global fits were still obtained.
- (33) Berecz, E.; Bader, I. *Acta Chim. Acad. Sci. Hung.*, 1973, 79, 81-103.
- (34) Haase, R.; Saurmann, P.F.; Duecker, K.H. *Z. Phys. Chem.*, 1965, 47, 224-225.
- (35) Xu, J.; Izvekov, S.; Voth, G.A. *J. Phys. Chem. B* 2010, 114, 9555
- (36) Lapid, H.; Agmon, N.; Petersen, M.K.; Voth, G.A. *J. Chem. Phys.* 2005, 122, 145
- (37) Wang, F.; Izvekov, S.; Voth, G.A. *J. Am. Chem. Soc.* 2008, 130, 3120

## TOC Graphics



## **Effect of cations on the hydrated proton**

Niklas Ottosson<sup>†</sup>, Johannes Hunger<sup>‡</sup> and Huib J. Bakker<sup>†</sup>

<sup>†</sup>*FOM Institute AMOLF, Science Park 104, 1098 XG Amsterdam, The Netherlands*

<sup>‡</sup>*Max Planck Institute for Polymer Research, Ackermannweg 10, D-55128 Mainz, Germany*

### **SI.1) Methods**

#### **SI.1.1 Dielectric relaxation measurements of aqueous electrolytes**

We measured the complex permittivities of various aqueous acid/salt mixtures in the range of 1 GHz to 50 GHz using a phase-sensitive vector network analyzer (VNA, Rhode-Schwartz model ZVA67) together with a home-built reflectometric cell for liquid samples.<sup>1</sup> We first calibrated the coaxial cable connecting the VNA to the sample cell with a commercial calibration kit (ZV-Z96, Rhode-Schwartz), using matched, open and short standards. Using these reference measurements we fitted the parameters of a three-term error model relating the emitted and reflected signals at the VNA measurement port.<sup>2</sup> We calibrated the set-up further by connecting the sample cell and measuring air, water and gold (short) as standards. The model of Blackham and Pollard was used to extract the complex permittivities from the measured scattering parameters of the liquid samples.<sup>3</sup> All measurements were performed at  $\sim 22 \pm 0.5^\circ\text{C}$ .

In an electrolyte, the dielectric function  $\hat{\epsilon}(\nu)$  can be thought of as having two frequency-dependent contributions, namely the dielectric function associated with the water solvent itself,  $\hat{\epsilon}_{\text{wat}}(\nu)$  and an additional susceptibility contribution,  $\chi_{\text{cond}}$ , arising from the conductivity of the mobile ionic charges in the electrolytes. From the Drude model,<sup>4</sup> the latter contribution can be approximated as  $\chi_{\text{cond}}(\nu) \approx i\sigma/\epsilon_0 2\pi\nu$ , in the limit  $\gamma^2 \gg \nu^2$ ; here  $\sigma$  is conductivity of the electrolyte,  $\epsilon_0$  is the vacuum permittivity, and  $\gamma$  is the damping constant of the moving charges (inversely proportional to their scattering time). The total measured dielectric response can thus be written as

$$\hat{\epsilon}(\nu) = \hat{\epsilon}_{\text{wat}}(\nu) + \chi_{\text{cond}}(\nu) \approx \hat{\epsilon}_{\text{wat}}(\nu) + \frac{i\sigma}{2\pi\nu\epsilon_0} \quad (\text{Eq. SI.1})$$

In the low frequency range of the present experiments on acid and salt solutions the imaginary part of the water Debye relaxation mode of electrolytes becomes small in comparison to the conductivity term of Eq. SI.1 which allows an accurate separation of the this contribution in the fitting. Thereafter the

conductivity dependent loss term can be removed from  $\hat{\epsilon}(\nu)$  upon which we retrieve  $\hat{\epsilon}_{\text{wat}}(\nu)$  associated with the water solvent.

### SI.1.2 Sample preparations

We prepared mixtures of inorganic salts  $YX_n$  ( $Y = \text{Cs, Na, Mg or Ca, } X = \text{Cl or ClO}_4$ ) and inorganic acids  $HX$  (where  $X = \text{Cl or ClO}_4$ ) volumetrically by mixing de-mineralized water (Millipore filtered, 18 M $\Omega$ ) with commercially obtained high purity salts (>99-99.5%, Sigma-Aldrich). All chemicals were used without further purification.

In order to systematically investigate the effect on the permittivity of acid and salt mixtures at different composition ratios and concentrations, we prepared sample series according to two different principles. In the first approach, series of mixtures of an acid  $HX$  and a salt  $YX_n$  was constructed such that the anion  $X^-$  concentration was held constant at either 0.1, 0.5 or 1 M. Nine solutions were then prepared where the composition was chosen such that  $[HX]:[YX_n]_n = 0:1, 0.125:0.875, 0.25:0.75, 0.375:0.625, 0.5:0.5, 0.625:0.375, 0.75:0.25, 0.875:0.125$  and 1:0. As a result, the cation composition spans linearly through mixtures of proton and salt cations, with the pure acid and salt solutions as the limiting cases. Since the anion concentration is the same throughout such a series, the effect of the anions on the dielectric spectra can be assumed to be similar. When  $\text{HCl}$  or  $\text{HClO}_4$  is co-solvated with a corresponding monovalent cationic salt, all solutions have the same ionic strength. However, in case  $\text{HCl}$  or  $\text{HClO}_4$  is co-solvated with salts of divalent cations, the ionic strength decreases by 1/3 upon going from the pure salt to the pure acid.

In the second approach a fixed concentration of 0.25M of  $\text{HCl}$  (or alternatively  $\text{MgCl}_2$ ) was added to solutions of variable concentrations of  $\text{MgCl}_2$  (or alternatively  $\text{HCl}$ ). Thus, in contrast to the first type of sample series, only the concentration of one component changes at a time. However, this means that both the anion concentration and the total ionic strength of the electrolyte are varied throughout the series.

Upon preparation, the densities of all samples were determined using a vibrating tube densitometer (LiquiPhysics Excellence DM40, Mettler Toledo). From the thus determined solution densities, the water concentrations were determined.

## SI.2) Data analysis

Figure 1 of the main article (as well as Figs. SI.4 – SI.7) presents the dielectric relaxation of water dipoles in mixed electrolytes after subtraction of the conductivity response, for increased visual clarity. However, the measured dielectric loss  $\epsilon''$  is dominated by the conductivity loss term  $\sigma/\epsilon_0\omega$ , especially for the HCl rich electrolytes. To demonstrate how this decomposition is done, Fig. SI.1 gives the measured raw data of mixed HCl/MgCl<sub>2</sub> electrolytes at 1 mol/L Cl<sup>-</sup> concentration. The top panel shows the real part which is not affected by the ionic conductivity (thus being identical to the top panel given in Fig. 1a in the main article). The middle part represents the total fit to  $\epsilon''$  given by Eq. 3 in the main text, whereas the bottom part shows the decomposition of  $\epsilon''$  into dielectric relaxation and conductivity contributions, i.e. given by the first and second term in the model used to fit all experimental data:

$$\hat{\epsilon}(\omega) = \frac{S}{1 + (i\omega\tau)^{1-\alpha}} + \epsilon_\infty - \frac{i\sigma}{2\pi\nu\epsilon_0} \quad (\text{Eq. SI.2})$$

In practice, in order to achieve similar weights in the fit of all data points over the entire frequency range, we first subtract the majority of the  $-i\sigma/2\pi\nu\epsilon_0$  term by assuming that the value of  $\epsilon''$  at 1 GHz is entirely due to conductivity. When fitting the resulting spectra we leave the remaining conductivity as a fit parameter in order to correct for small differences between the initially subtracted  $i\sigma/2\pi\nu\epsilon_0$  term and the actual sample conductivity response.

To reduce the number of fitting parameters,  $\epsilon_\infty$  was fixed to the value for neat water,<sup>5</sup> leaving only  $S$ ,  $\tau$ ,  $\alpha$  and  $\sigma$  as fit parameters. In tables SI.1 and SI.2 we present examples of extracted fit parameters for MgCl<sub>2</sub>/CsCl and MgCl<sub>2</sub>/HCl mixtures, respectively (corresponding to the data in Fig. 1 in main article). There are only small variations in  $\tau$ , which for the MgCl<sub>2</sub>/CsCl mixtures runs smoothly between the limiting values of the pure 0.5M MgCl<sub>2</sub> and 1M CsCl electrolytes. For the MgCl<sub>2</sub>/HCl mixtures there is a very slight increase in  $\tau$  at intermediate compositions. For all solutions the  $\alpha$ -parameter, describing the broadening of the Cole-Cole relaxation mode, is close to zero, i.e. all modes are close to a simple Debye mode. As expected, for both salt-salt and salt-acid mixtures the broadening is the largest at intermediated compositions, due to the increased inhomogeneity of the sample. Even in this case the line shape remains very close to that of a Debye mode.

**Table SI.1) Fit parameters of MgCl<sub>2</sub>/CsCl mixtures at 1 mol/l Cl<sup>-</sup>. Note that conductivities  $\sigma$  refer to total conductivities extracted (i.e. the initially subtracted value + residual fit value).**

$2[MgCl_2]:[CsCl]$	$\epsilon_S$	$\tau$ [ps]	$\alpha$	$\sigma$ [S/m]
1:0	66.63	8.65	0.027	6.76
0.875:0.125	67.31	8.60	0.028	7.30
0.75:0.25	67.98	8.59	0.029	7.71
0.625:0.375	68.59	8.52	0.029	8.14
0.5:0.5	69.16	8.48	0.029	8.65
0.375:0.625	69.70	8.44	0.030	9.14
0.25:0.75	70.29	8.37	0.030	9.59
0.125:0.875	70.79	8.30	0.029	10.1
0:1	71.33	8.23	0.028	10.6

**Table SI.2) Fit parameters of MgCl<sub>2</sub>/HCl mixtures at 1 mol/l Cl<sup>-</sup>. Note that conductivities  $\sigma$  refer to total conductivities extracted (i.e. the initially subtracted value + residual fit value).**

$2[MgCl_2]:[HCl]$	$\epsilon_S$	$\tau$ [ps]	$\alpha$	$\sigma$ [S/m]
1:0	66.69	8.73	0.029	6.76
0.875:0.125	66.49	8.83	0.034	9.50
0.75:0.25	65.64	8.88	0.037	12.4
0.625:0.375	64.45	8.88	0.037	15.4
0.5:0.5	62.85	8.85	0.033	18.7
0.375:0.625	61.30	8.86	0.031	21.8
0.25:0.75	59.38	8.78	0.028	25.1
0.125:0.875	57.47	8.70	0.024	28.5
0:1	55.59	8.63	0.021	31.9

From the fits the total dielectric strength  $S$  associated with the orientational relaxation of water molecules in a given electrolyte is obtained. For all investigated electrolytes the amplitude  $S$  is smaller for aqueous electrolytes than that of pure water. Only a small part of this difference is due to the dilution of water upon addition of the salt and/or acid; an effect that is corrected for by comparing the apparent water concentration with the analytical water concentration in the solution (obtained from density measurements). In tables SI.3 and SI.4 we present examples of measured densities and derived water concentrations of MgCl<sub>2</sub>/CsCl and MgCl<sub>2</sub>/HCl mixtures, respectively (corresponding to the data in Fig. 1 in main article).

**Table SI.3) Densities and water concentrations of mixed MgCl<sub>2</sub>/CsCl electrolytes at 1 mol/l Cl<sup>-</sup>.**

$2[MgCl_2]:[CsCl]$	$\rho$ [kg/dm <sup>3</sup> ]	$c_{H_2O}$ [mol/L]
1:0	1.0353	55.0
0.875:0.125	1.0464	54.8
0.75:0.25	1.0575	54.5
0.625:0.375	1.0685	54.3
0.5:0.5	1.0796	54.1
0.375:0.625	1.0907	53.9
0.25:0.75	1.1018	53.7
0.125:0.875	1.1128	53.4
0:1	1.1239	53.2

**Table SI.4) Densities and water concentrations of mixed MgCl<sub>2</sub>/HCl electrolytes at 1 mol/l Cl<sup>-</sup>.**

$2[MgCl_2]:[HCl]$	$\rho$ [kg/dm <sup>3</sup> ]	$c_{H_2O}$ [mol/L]
1:0	1.0353	55.0
0.875:0.125	1.0327	54.9
0.75:0.25	1.0303	54.9
0.625:0.375	1.0275	54.8
0.5:0.5	1.0249	54.7
0.375:0.625	1.0223	54.7
0.25:0.75	1.0197	54.6
0.125:0.875	1.0166	54.5
0:1	1.0144	54.5

In the main text we defined the depolarization as  $\Delta S = S_n - S$ , where  $S_n$  is the water density corrected dielectric response (using the Cavell equation) that would nominally be expected if the orientational freedom of the water molecules in the solution was the same as that of pure water. Figure SI.2 shows an example (for HCl/MgCl<sub>2</sub> mixtures at 1 mol/L Cl<sup>-</sup> concentration, corresponding to the permittivity data given in Fig. 1a in the main text) of how the depolarization  $\Delta S$  is derived from the difference  $S_n - S$ .

### SI.3) Conductivity data and kinetic depolarization

Figures SI.3 shows conductivity data for the mixed HCl/MgCl<sub>2</sub> electrolytes for which  $\Delta S$  and  $c_{\text{aff}}$  values were given in Fig. 3 of the main text. While the ionic strengths of these electrolytes are too high for Debye-Hückel theory (and thus Kohlrausch law) to be quantitatively applicable, we can still well fit the conductivity of the MgCl<sub>2</sub>/HCl solutions to the expression:

$$\sigma = [\text{MgCl}_2](A - B\sqrt{I_{\text{tot}}}) + [\text{HCl}](C - D\sqrt{I_{\text{tot}}}) \quad (\text{Eq. SI.3})$$

The resulting fit is shown as solid lines together with the measurement data in Fig. SI.3.

The translational motion of ions in solution, which is quantified by the solution's conductivity, gives rise to a kinetic depolarization contribution to the dielectric response. The contribution of the kinetic depolarization can be calculated from the dielectric parameters of the solvent and the conductivity of the electrolyte using the continuum theory of Hubbard and Onsager<sup>6</sup>. Buchner and co-workers have successfully applied this theory, using slip hydrodynamic boundary conditions, in previous dielectric studies of electrolyte solutions.<sup>5</sup> Following that strategy, the part  $\Delta S_{\text{KD}}$  of the total depolarization  $\Delta S$  that originates from kinetic depolarization is obtained as:

$$\Delta S_{\text{KD}} = \sigma \frac{2}{3} \frac{\varepsilon(0) - \varepsilon_{\infty}(c)}{\varepsilon(0)} \frac{\tau_{\text{D}}(0)}{\varepsilon_0}. \quad (\text{Eq. SI.4})$$

Using the same approach as in Eq. 2 in the main text we derive  $c_{\text{KD}} = \Delta S_{\text{KD}} \times c_0/S_0$ . Thereby we can determine the normalized difference  $Z_{\text{IB}} = (c_{\text{aff}} - c_{\text{KD}})/c$ , (where  $c$  is the concentration of the electrolyte) from the measurements of the pure salt solutions (NaCl, CsCl, MgCl<sub>2</sub>, and HCl). It has been shown previously, that these  $Z_{\text{IB}}$  values represent the hydration number of strongly bound water molecules in the hydration shell of the cations, as the contribution of the anionic hydration shell for Cl<sup>-</sup> and ClO<sub>4</sub><sup>-</sup> can be neglected.<sup>5, 7</sup> The thus obtained cation coordination numbers for the pure electrolytes studied here,  $Z_{\text{IB}}(\text{Na}^+) = 5 \pm 0.5$ ,  $Z_{\text{IB}}(\text{Cs}^+) = 0 \pm 0.5$ ,  $Z_{\text{IB}}(\text{H}^+) = 4 \pm 0.5$ ,  $Z_{\text{IB}}(\text{Ca}^+) = 11 \pm 1$  and  $Z_{\text{IB}}(\text{Mg}^+) = 13 \pm 1$ , at 1 mol/L Cl<sup>-</sup> concentrations, are in good agreement with previous reports in the literature.<sup>5, 7-8</sup>

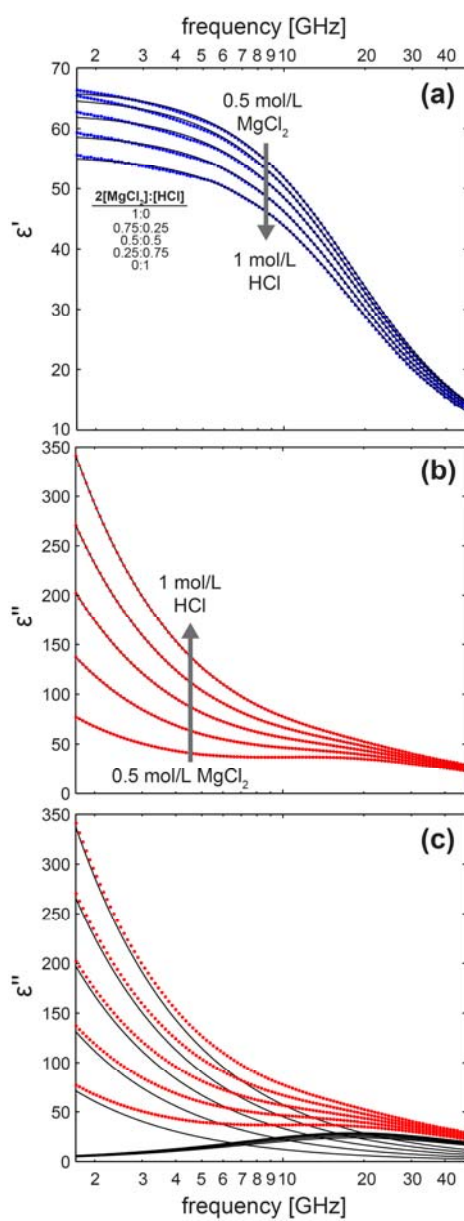
#### SI.4) Additional data

While the primary focus of this study is on the HCl/MgCl<sub>2</sub>/H<sub>2</sub>O ternary system, comparisons were done against reference systems of HCl/CaCl<sub>2</sub>/H<sub>2</sub>O, HClO<sub>4</sub>/Mg(ClO<sub>4</sub>)<sub>2</sub>/H<sub>2</sub>O and HCl/CsCl/H<sub>2</sub>O which were referred to in the main article. Figure SI.4a) gives raw permittivity spectra for different mixtures from 1 mol/L HCl and 0.5 mol/L CaCl<sub>2</sub>, i.e. the series is constructed analogous to those given in Fig. 1 and 2 of the main paper. Similarly, panel b) shows data from mixtures of 1 mol/L HClO<sub>4</sub> and 0.5 mol/L Mg(ClO<sub>4</sub>)<sub>2</sub>. The extracted  $\Delta S$  and  $c_{\text{aff}}$  values from these data are plotted in panel c), together with that of the 1mol/L HCl / 0.5 mol/L MgCl<sub>2</sub> system from Fig. 2 of the main paper. If the specific nature of the Mg<sup>2+</sup> cation would have been the main reason behind the non-linearity in  $\Delta S$  and  $c_{\text{aff}}$  as function of composition we would have expected the HCl/MgCl<sub>2</sub> and HCl/CaCl<sub>2</sub> curves to be considerably different, with the latter giving a more linear dependence upon variation of composition. Similarly, if the specific nature of the Cl<sup>-</sup> anion was the source of the effect we would expect a pronounced difference between the HCl/MgCl<sub>2</sub> and HClO<sub>4</sub>/Mg(ClO<sub>4</sub>)<sub>2</sub> data. Since the differences between the three series are small we can exclude both these scenarios.

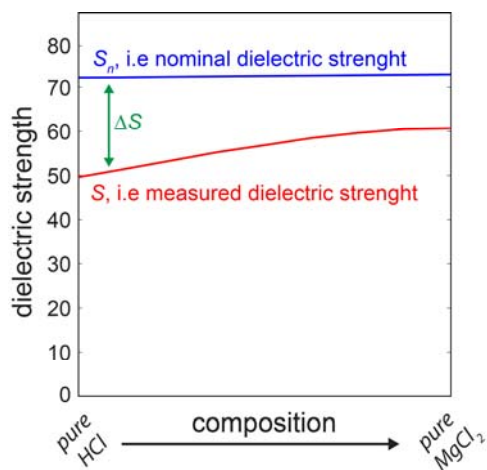
As argued for in the main article, the dominating factor for the non-linearity in  $\Delta S$  and  $c_{\text{aff}}$  rather seems to be the valency of the cation co-solvated with the proton. This can indeed be seen in figure SI.5 where mixture data for HCl and CsCl is shown. Panel a) gives raw permittivity data for mixtures with at 1 and 0.5 mol/L Cl<sup>-</sup> concentration. Panel b) in turn gives the extracted  $\Delta S$  and  $c_{\text{aff}}$  values; the circles give experimental data points while the solid lines are fits to Eq. 2 in the main article. The non-linearity across the composition range is very weak, if at all present – the fitted values are  $A = 5 \text{ L/mol}$ ,  $B = 23 \text{ L/mol}$  and  $C = 4 \text{ L}^2/\text{mol}^2$ .

Finally, Figs. SI.6 and SI.7 gives raw permittivity spectra for electrolytes with varying concentration of HCl (SI.6) and MgCl<sub>2</sub> (SI.7), from which the  $\Delta S$  and  $c_{\text{aff}}$  values in Fig. 4 of the main article were extracted. In the a) panels of each figure, data for pure the pure binary systems (HCl and MgCl<sub>2</sub>, respectively) are given at various concentrations. The b) panels gives the corresponding data for systems which a fixed 0.25 mol/L concentration of the other component, i.e. MgCl<sub>2</sub> in 4b) and HCl in 5b), was added.

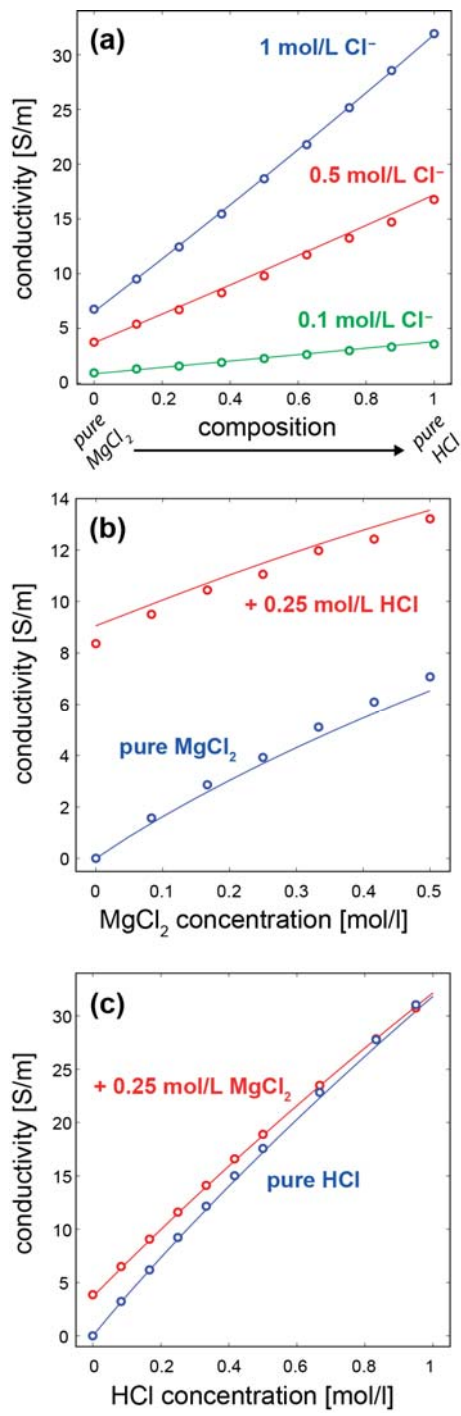
## SI Figures



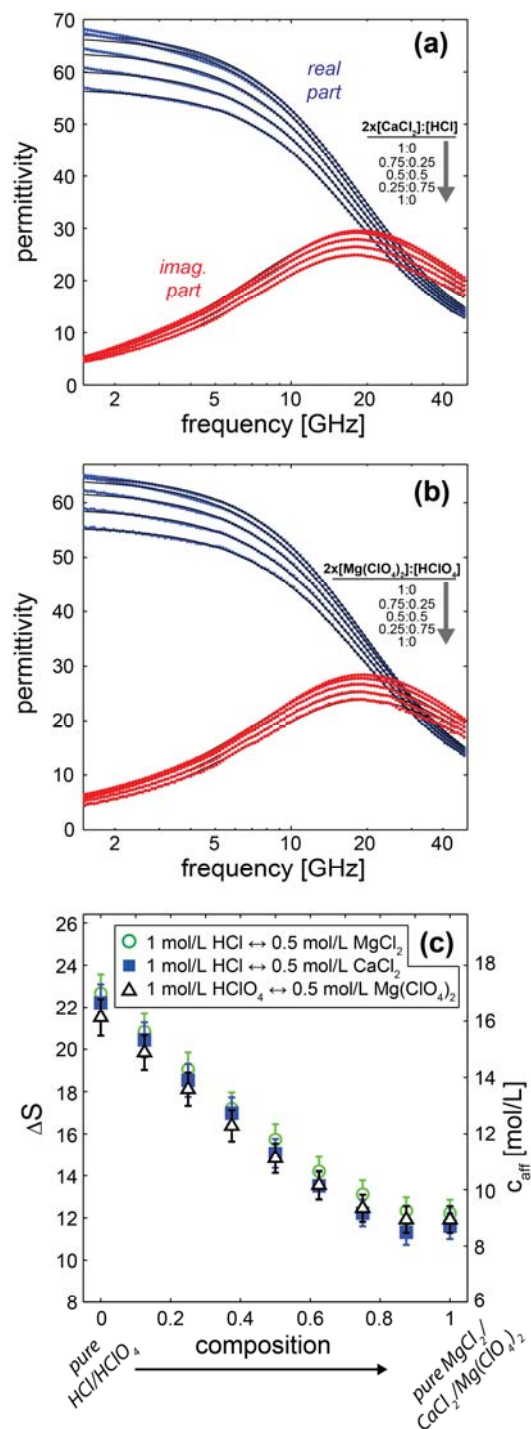
**SI Figure 1)** Measured raw data of mixed HCl/ $\text{MgCl}_2$  electrolytes at 1 mol/L  $\text{Cl}^-$  concentration. Panel a) panel shows the real part which is not affected by the ionic conductivity (thus being identical to the top panel given in Fig. 1a in the main article). The middle part represents the total fit to  $\epsilon''$  given by Eq. 3 in the main text, whereas the bottom part shows the decomposition of  $\epsilon''$  into dielectric relaxation and conductivity contributions.



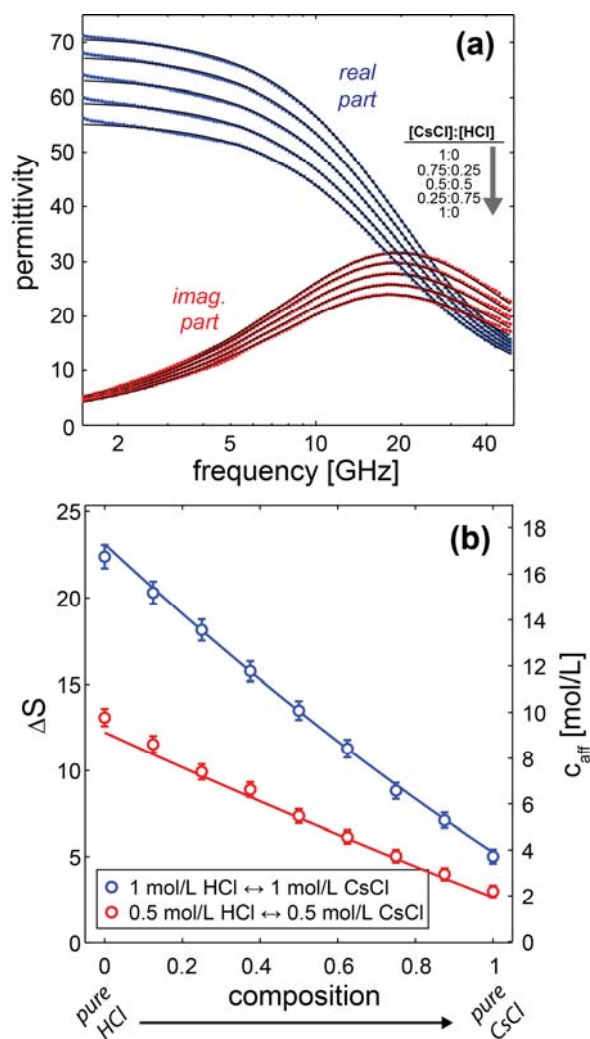
**SI Figure 2)** Plot of how the depolarization  $\Delta S$  is derived from the difference  $S_n - S$ , i.e. that between the nominal dielectric response  $S_n$  expected if all water molecules in the sample contributed to the dielectric relaxation and the measured dielectric strength  $S$ . The data corresponds to mixtures of HCl/MgCl<sub>2</sub> at 1 mol/L Cl<sup>-</sup>, i.e the permittivity data given in Fig. 1a in the main text.



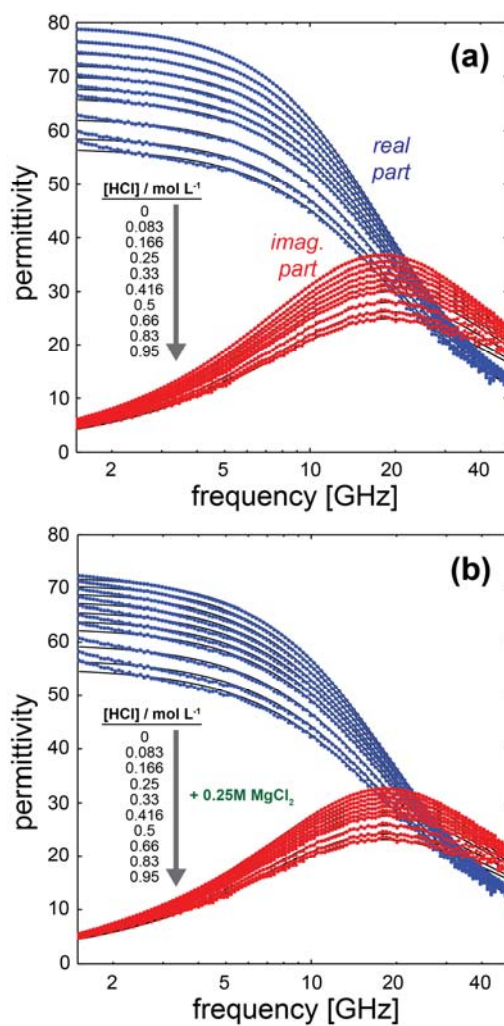
**SI Figure 3)** Conductivities of mixed  $\text{MgCl}_2/\text{HCl}$  solutions of which the  $\Delta S$  and  $c_{\text{aff}}$  values are given in Fig. 3 of the main manuscript. Solid lines are fits to SI Eq. 4.



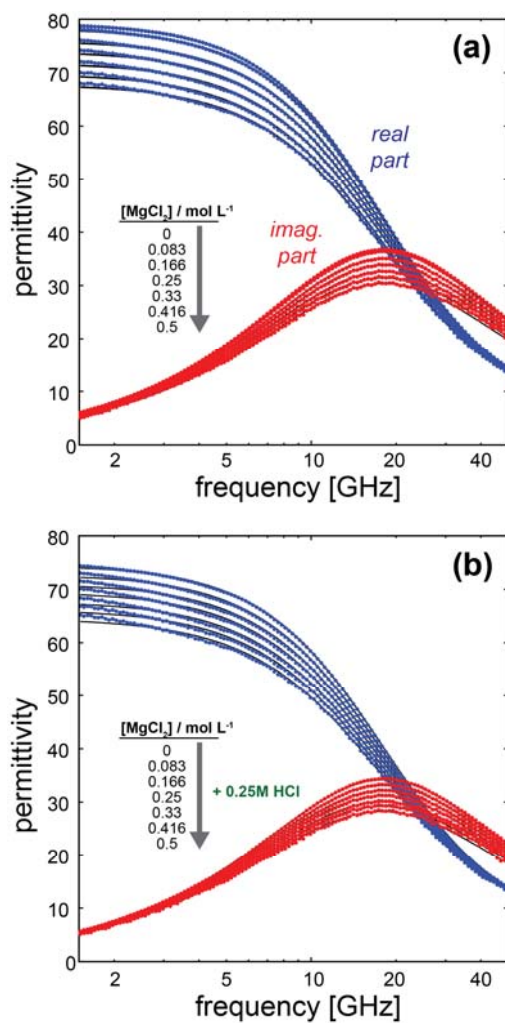
**SI Figure 4)** Conductivity-corrected permittivity spectra of a) 1 mol/L HCl / 0.5 mol/L CaCl<sub>2</sub> mixtures and b) 1 mol/L HClO<sub>4</sub> / 0.5 mol/L Mg(ClO<sub>4</sub>)<sub>2</sub> mixtures. Panel c) shows the extracted  $\Delta S$  and  $c_{\text{aff}}$  values for these systems, plotted together with those of 1 mol/L HCl / 0.5 mol/L MgCl<sub>2</sub> (as given in Fig. 4 in the main article).



**SI Figure 5)** Panel a) gives conductivity-corrected permittivity spectra of 1 mol/L HCl / 1 mol/L CsCl. Panel b) shows extracted experimental  $\Delta S$  and  $c_{\text{aff}}$  values for mixtures at 1 mol/L (blue circles) and 0.5 mol/L (red circles) together with least-square fits (solid lines) to Eq. 3 in the main article.



**SI Figure 6)** Panel a) gives conductivity-corrected permittivity spectra of HCl electrolytes at various concentrations, up to 0.95 mol/L. Data for the same concentrations of HCl, co-solvated with 0.25 mol/L MgCl<sub>2</sub> is given in panel b).



**SI Figure 7)** Panel a) gives conductivity-corrected permittivity spectra of MgCl<sub>2</sub> electrolytes at various concentrations, up to 0.5 mol/L. Data for the same concentrations of MgCl<sub>2</sub>, co-solvated with 0.25 mol/L HCl is given in panel b).

## SI References

1. Ensing, W.; Hunger, J.; Ottosson, N.; Bakker, H. J., *J. Phys. Chem. C* **2013**, *117*, 12930-12935.
2. Hiebel, M., *Fundamentals of Vector Network Analysis*. Rohde & Schwarz GmbH: 2007.
3. Blackham, D. V.; Pollard, R. D., *IEEE Trans. Instrum. Meas.* **1997**, *46*, 1093 – 1099.
4. Ashcroft, N. W.; Mermin, N. D., *Solid State Physics*. Saunders College: 1976.
5. Buchner, R.; Hefter, G. T.; May, P. M., *J. Phys. Chem. A* **1999**, *103* (1), 1-9.
6. (a) Hubbard, J.; Onsager, L., *J. Chem. Phys.* **1977**, *67*, 4850; (b) Hubbard, J.; Onsager, L.; Beek, W. M. v.; Mandel, M., *Proc. Nat. Ac. Sci.* **1977**, *74*, 401.
7. Tielrooij, K. J.; Garcia-Araez, N.; Bonn, M.; Bakker, H. J., *Science* **2010**, *328*, 1006-1009.
8. (a) Chen, T.; Hefter, G.; Buchner, R., *J. Phys. Chem. A* **2003**, *107*, 4025-4031; (b) Buchner, R.; Chen, T.; Hefter, G., *J. Phys. Chem. B* **2004**, *108*, 2365-2375; (c) Tielrooij, K. J.; Timmer, R. L. A.; Bakker, H. J.; Bonn, M., *Phys. Rev. Lett.* **2009**, *102*, 198303.